Available online at www.sciencedirect.com
ScienceDirect
Journal of Hazardous Materials 147 (2007) 363–369
Journal of Hazardous Materials
www.elsevier.com/locate/jhazmat

Study of the separation efficiency of a demister vane with response surface methodology

Jianzhi Zhao, Baosheng Jin*, Zhaoping Zhong

Key Laboratory of Clean Coal Power Generation and Combustion Technology of Ministry of Education, Thermo-Energy Engineering Research Institute, Southeast University, Nanjing 210096, China

Received 3 July 2006; received in revised form 2 September 2006; accepted 4 January 2007
Available online 19 January 2007

Abstract

Numerical simulations of a demister vane with various geometries and operating conditions were performed to study the separation efficiency. The numerical solutions were carried out using commercial CFD code Fluent 6.1. A prediction model of the separation efficiency was obtained based on response surface methodology by means of the statistical software program Minitab V14. The results show that not only the vane spacing and flue gas velocity, but also vane height (including height of curve and upright region) and vane turning angles, play an important role in influencing the separation efficiency. Compared with some experimental and simulative conclusions, the results indicate that present prediction model can estimate the effects of different geometries and operation conditions on the separation efficiency, and can direct the optimum design of demisters.

Keywords: Response surface methodology; Numerical simulation; Demister; Separation efficiency

1. Introduction

There are some methods used for demisting of gases and vapors including settling tanks [1], fiber filtering candles [2], electrostatic precipitators [3], cyclones, wire mesh and demister. Demister is one of the most interesting equipments in the wet flue gas desulphurization (WFGD) system. It is assembled in the out let of the desulphurization tower by capturing the liquid droplets of the flue gas. Separation efficiency is an important parameter to evaluate the performance of a demister. It will influence the good running of WFGD directly. The separation efficiency was investigated by Bradie and Dickson [4] and Claes and De Bruyne [5]. Presently, some researchers have studied this parameter to improve the performance of demisters [6–13]. However, determining the influence of different geometries and operation conditions on the separation efficiency by means of experiments will expenses and difficulty. On the other hand, with the rapid development of the computer and computational fluid dynamics (CFD) techniques, the use of numerical simulations to predict the performance of the demister has received much attention and it is at present under intensive development [14–17]. An evident advantage of CFD calculations with respect to experiments is that a large number of geometry variables can be varied at relative low costs [18,19]. In this work, CFD calculations are used instead of experiments to relate the separation efficiency with the structural parameters of a demister.

Response surface methodology (RSM) a fractional factorial CFD calculations designs, provides a systematic and efficient research strategy for studying the parameter effect using statistical methods. It has been extensively applied in industrial fields in recent years [20–23]. Response surface methodology permits efficient experimental investigation of the response of a system to concurrent variations in any number of independent variables. This technique produces an empirical equation describing the response and a statistical assessment of the adequacy of the description.

The present work is an attempt to study the separation efficiency of an undee demister vane using RSM, aiming at determining the relationship among the separation efficiency, geometries and operating conditions. An equation is derived,

* Corresponding author. Tel.: +86 25 83794744; fax: +86 25 83795508.
E-mail address: bsjin@seu.edu.cn (B. Jin).

0304-3894/$ – see front matter © 2007 Published by Elsevier B.V.
doi:10.1016/j.jhazmat.2007.01.046

Nomenclature

C_D	The drag coefficient
d_p	the droplets diameter (m)
D	The vane spacing (mm)
H_1	height of the vane upright region (mm)
H_2	height of the vane curve region (mm)
Re	the relative Reynolds number
u	the gas phase velocity ($m\,s^{-1}$)
u_p	the droplets velocity ($m\,s^{-1}$)
v	the flue gas velocity ($m\,s^{-1}$)
X_{iH}	the high levels of the ith factor
X_{iL}	the low levels of the ith factor
$\bar{X}_i$	the mean levels of the ith factor
X_0	the CFD calculation quantity
X_p	the predicted quantity

Greek letters

α	the vane turning angles (°)
μ	the molecular viscosity of gas phase ($m^2\,s^{-1}$)
ρ	the gas phase density ($kg\,m^{-3}$)
ρ_p	the density of droplets ($kg\,m^{-3}$)

which relates these variables with the separation efficiency. This model can be used for optimizing the design at a required performance level.

2. Model set-up

2.1. Response surface design

Provided that the response surface is adequately fit by a second-order model, the estimated response Y for input k variables is given by Hinkelmann and Kempthorne [24]:

$$Y = \beta_0 + \sum_{i=1}^{k}\beta_i x_i + \sum_{i=1}^{k}\beta_{ii}x_i^2 + \sum_{i<j}\beta_{ij}x_i x_j + e(x_1, x_2, ..., x_k) \quad (1)$$

where x_i is the level setting of factor i, β_i, β_{ii} and β_{ij} represent regression coefficients for the linear, quadratic and interaction terms, and e is the error. There are two sources of error, viz. an experimental error, and a lack-of-fit error; the latter incorporates higher order terms or interactions. It was not possible to estimate the experimental error due to the deterministic character of the CFD model applied in this study; as a result, the error term only relates to the model capability.

It is assumed that the performance of a demister vane is affected by at least five factors, viz. α, H_1, H_2, D, and v, as shown in Fig. 1. A way to estimate the parameters of Eq. (1) is to study the response for all (combinations of) factors set at three different levels. This full factorial design would require $3^5 = 243$ different CFD simulations. However, the number of degrees of freedom (d.f.) of the second-order model is only $2k + 1/2k(k-1)$, which is equal to 20 for a five-factor design. A more suitable design to estimate the regression coefficients with a limited number of

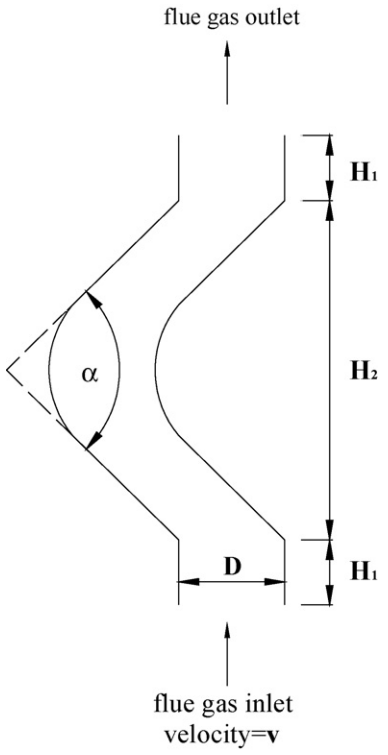

Fig. 1. Structural schematic of a demister vane.

points of the central composite design were located on a face centred hypercube [25], which is composed of three parts: (1) a full factorial part of 2^k vertices; (2) an axial part of $2k$ points at the origin of each factors axis; and (3) a center point [26]. These set-up results in a central composite design of five factors demanding only 43 CFD calculations, which is a considered reduction compared to the three level factorial design. A three-factor central composite design is illustrated in Fig. 2.

The regression coefficients of Eq. (1) are estimated by means of a least squares method. Since the variance of the model parameters depends on both the mean square error (M.S.E.) and the factor magnitude, it is convenient to scale the factor level as follows:

$$x_i = \frac{X_i - \bar{X}_i}{(1/2)(X_{iH} - X_{iL})} \quad (2)$$

where X_{iH} and X_{iL} denote the high and low level of the ith factor, respectively, and $\bar{X}_i$ is the mean level. In coded units, the high

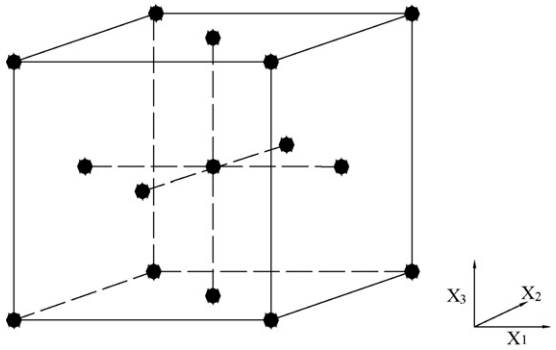

Fig. 2. A three-factor central composite design.

and low levels become $X_{i\mathrm{H}} = 1$ and $X_{i\mathrm{L}} = -1$, respectively, and the mean factor level, $\bar{X}_i$, is equal to zero. Coded factor levels are used in the so-called design-model matrix, which represents all points needed in the central composite design.

2.2. CFD model

Considering the reasonability of the time counting, we make the below presumption during the process of modeling:

(1) The ratio of the breadth and the height of the demister vane is big enough to simplify the inside flow field as two-dimension.
(2) The number of the vanes is reduced during the model process based on the consideration of the reasonability of the time counting.
(3) The velocity of the flue gas inside the demister vane is slow enough (≤6 m/s) to assume that the flue gas is non-compressible gas.
(4) The diameter of the liquid droplets is short enough to assume them as sphere and the diameter is stable during their movements. The drag of the gas phase and the gravity is considered.
(5) The liquid drops are considered captured as soon as they crash into the wall of the route-way, neglecting the influences of the rebound and film above the wall.
(6) The liquid drops are considered escaped as soon as they leave the out-let of the demister.

2.2.1. Construction of the model

In a two-dimension Euler system of coordinates, the flow filed of flue gas is calculated, using the SIMPLE algorithm. The movement of liquid droplets is calculated by Lagrange method.

The continuous equation, Navier–Stokes equation and $k-\varepsilon$ equation of continuous phase is described as:

$$\frac{\partial u}{\partial x} + \frac{\partial v}{\partial y} = 0 \tag{3}$$

$$\frac{\partial u}{\partial t} + u\frac{\partial u}{\partial x} + v\frac{\partial u}{\partial y} = Fx - \frac{\partial p}{\partial x} + \frac{1}{Re}\left[\frac{\partial^2 u}{\partial x^2} + \frac{\partial^2 u}{\partial y^2}\right] \tag{4}$$

$$\frac{\partial v}{\partial t} + u\frac{\partial v}{\partial x} + v\frac{\partial v}{\partial y} = Fx - \frac{\partial p}{\partial y} + \frac{1}{Re}\left[\frac{\partial^2 v}{\partial x^2} + \frac{\partial^2 v}{\partial y^2}\right] \tag{5}$$

$$\frac{\partial}{\partial t}(\rho k) + \frac{\partial}{\partial x_j}(\rho k u_j) = \frac{\partial}{\partial x_j}\left[\left(\mu + \frac{\mu_t}{\sigma_k}\right)\frac{\partial k}{\partial x_j}\right] + \mu\frac{\partial u_i}{\partial x_j}\left[\frac{\partial u_i}{\partial x_j} + \frac{\partial u_j}{\partial x_i}\right] - \rho\varepsilon \tag{6}$$

$$\frac{\partial}{\partial t}(\rho\varepsilon) + \frac{\partial}{\partial x_k}(\rho\varepsilon u_k) = \frac{\partial}{\partial x_k}\left[\left(\mu + \frac{\mu_t}{\sigma_\varepsilon}\right)\frac{\partial \varepsilon}{\partial x_k}\right] + \frac{c_1\varepsilon}{k}\mu\frac{\partial u_i}{\partial x_j}\left(\frac{\partial u_i}{\partial x_j} + \frac{\partial u_j}{\partial x_i}\right) - c_2\rho\frac{\varepsilon^2}{k} \tag{7}$$

where μ_t is turbulent velocity and is calculated as [27]:

$$\mu_t = \frac{c_\mu \rho k^2}{\varepsilon} \tag{8}$$

With $c_\mu = 0.09$, $c_1 = 1.44$, $c_2 = 1.92$, $\sigma_k = 1.0$, $\sigma_\varepsilon = 1.3$.

The particle trajectory is calculated by integrating the stress equation of liquid droplets in Lagrange system of coordinates.

Motion equation of liquid droplets is described by [28]:

$$\frac{du_\mathrm{p}}{dt} = F_\mathrm{D}(u - u_\mathrm{p}) + \frac{g_x(\rho_\mathrm{p} - \rho)}{\rho_\mathrm{p}} + Fx \tag{9}$$

With $F_\mathrm{D}(u - u_\mathrm{p})$ is the unit drag of liquid droplets and is calculated as:

$$F_\mathrm{D} = \frac{18\mu}{\rho_\mathrm{p} d_\mathrm{p}^2}\frac{C_\mathrm{D} Re}{24} \tag{10}$$

where u is the gas phase velocity, u_p the droplets velocity, μ the molecular viscosity of the gas phase, ρ the gas phase density, ρ_p the density of the droplets, and d_p is the droplets diameter. Re is the relative Reynolds number, which is defined as follows:

$$Re \equiv \frac{\rho d_\mathrm{p}\left|u_\mathrm{p} - u\right|}{\mu} \tag{11}$$

The drag coefficient, C_D, can be taken from [29]:

$$C_\mathrm{D} = \begin{cases} \dfrac{24}{Re}, & Re \le 1 \\ (1 + Re2/3/6)24/Re, & 1 < Re < 1000 \\ 0.44, & Re \ge 1 \end{cases} \tag{12}$$

2.2.2. Boundary condition of the model

The quad grid is applied to generate the mesh of the calculated vane. The inlet condition of gas phase is the velocity-inlet. The enter velocity of liquid droplets is assumed to be equal to the inlet velocity of flue gas. The outlet condition is outflow. The particle size distribution of droplets is according to the data of an electric power plant and assumed to be agreed with the Rosin–Rammler diameter distribution. The minimal diameter is 10 μm and the maximum one is 40 μm. The mean diameter of droplets is 21 μm, and the spread parameter is 3.77. It is considered the droplets are trapped when they crash into the wall.

2.2.3. Acquisition of the results

Assume that there are n kinds of liquid droplets with different diameter and the number of the droplets (d_i) is x_i, and the number of those captured by the wall is y_i. Then the separation efficiency of the droplets (d_i) is $\eta_{d_i} = y_i/x_i$. Assume the total weight of the droplets (d_i) is m_i, then the total separation efficiency is calculated as:

$$\eta = \frac{\sum_{i=1}^{n}(m_i\eta_{d_i})}{\sum_{i=1}^{n} m_i} \tag{13}$$

2.2.4. Comparison of model simulations with experimental data

In Lang et al. [9], a pilot-scale plant was built to experiment the separation efficiency of a demister vane. The mean diameter

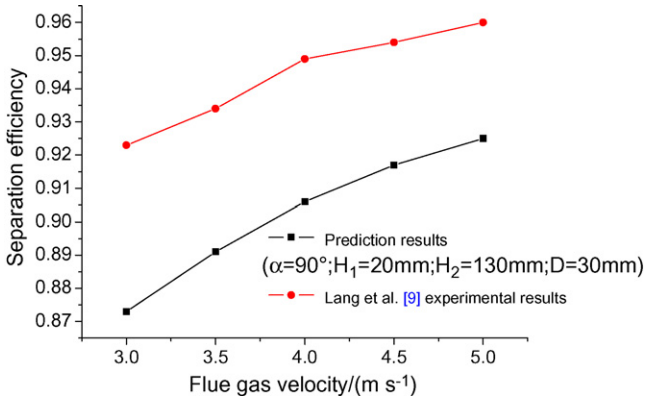

Fig. 3. Comparison of the published experimental and model calculated of separation efficiency at various flue gas velocities.

Table 1
Low and high level settings of the factors used in the response surface model

Factor	x_i	X_{iL}	X_{iH}
α (°)	x_1	60	120
H_1 (mm)	x_2	10	30
H_2 (mm)	x_3	120	140
D (mm)	x_4	25	35
v (m/s)	x_5	3	5

of droplets of Lang's experiment was 50 μm. Operation of the demister vane is modeled to verify the model. A comparison of modeled and experimentally measured dependence of separation efficiency to flue gas velocity is presented in Fig. 3. The results show that calculations agree well with the published experiments.

2.3. Responses and factors

In Table 1, the high and low levels of the geometries and operating parameters are presented. The coded factor levels correspond to −1, 0, and 1 according to Eq. (2), and the factors are denoted by x_i.

3. Results and discussion

3.1. Analysis of variance for the whole model

The results of the CFD predictions on the separation efficiency are summarized in Table 2.

The corresponding analysis of variance is tabulated in Table 3. The extremely small probability value (far smaller than 0.050) indicates that the calculation data are fitted well by the quadratic model, which is much higher than the 95% confidence level.

Via the multiple regression, a polynomial quadratic model or called a second-order response surface model was obtained as following:

$$Y = 1.95539 + 0.004491X_1 + 0.001046X_2 - 0.02186X_3 - 0.0074X_4 + 0.182297X_5 - 0.00004X_1^2 + 0.000057X_2^2 + 0.00008X_3^2 + 0.000001X_4^2 - 0.001033X_5^2 - 0.000003X_1X_2 + 0.000013X_1X_3 - 0.000043X_1X_4 - 0.00047X_1X_5 + 0.000005X_2X_3 + 0.00001X_2X_4 - 0.00053X_2X_5 + 0.000038X_3X_4 - 0.00015X_3X_5 - 0.00069X_4X_5 \quad (14)$$

Table 2
Central composite design of separation efficiency

No.	X_1	X_2	X_3	X_4	X_5	Y
1	60	10	120	25	3	0.8431
2	120	10	120	25	3	0.5908
3	60	30	120	25	3	0.8862
4	120	30	120	25	3	0.6415
5	60	10	140	25	3	0.8538
6	120	10	140	25	3	0.6239
7	60	30	140	25	3	0.9
8	120	30	140	25	3	0.6892
9	60	10	120	35	3	0.7494
10	120	10	120	35	3	0.5367
11	60	30	120	35	3	0.8078
12	120	30	120	35	3	0.5767
13	60	10	140	35	3	0.7622
14	120	10	140	35	3	0.5494
15	60	30	140	35	3	0.81
16	120	30	140	35	3	0.5806
17	60	10	120	25	5	0.8931
18	120	10	120	25	5	0.6315
19	60	30	120	25	5	0.9116
20	120	30	120	25	5	0.6638
21	60	10	140	25	5	0.8831
22	120	10	140	25	5	0.6385
23	60	30	140	25	5	0.9038
24	120	30	140	25	5	0.6515
25	60	10	120	35	5	0.8178
26	120	10	120	35	5	0.4839
27	60	30	120	35	5	0.8372
28	120	30	120	35	5	0.5111
29	60	10	140	35	5	0.8128
30	120	10	140	35	5	0.5272
31	60	30	140	35	5	0.8706
32	120	30	140	35	5	0.5506
33	60	20	130	30	4	0.836
34	120	20	130	30	4	0.5973
35	90	10	130	30	4	0.742
36	90	30	130	30	4	0.7747
37	90	20	120	30	4	0.76
38	90	20	140	30	4	0.7613
39	90	20	130	25	4	0.7954
40	90	20	130	35	4	0.71
41	90	20	130	30	3	0.724
42	90	20	130	30	5	0.7607
43	90	20	130	30	4	0.7393

Performance analysis of the response surface model is made by comparing model outputs with CFD calculation values at certain trials. The comparison was carried out by estimating the following statistical performance measures [30,31]:

Geometric mean bias (MG):

$$\mathrm{MG} = \exp\overline{(\ln X_0 - \ln X_p)} \quad (15)$$

Table 3
Corresponding analysis of variance of second-order model

Source	d.f.	Seq SS	Adj MS	*F*-Ratio	*P*-Value
Regression	20	0.651966	0.032598	112.16	0.000
Linear	5	0.633876	0.126775	436.19	0.000
Square	5	0.008464	0.001693	5.82	0.000
Interaction	10	0.009627	0.000963	3.31	0.000
Residual error	22	0.006394	0.000291		
Total	42	0.658361			

Table 4
Statistical performance measures calculated for the predicted model

Statistical measures	MG	VG
Ideal value	1	1
Dispersion model	0.944	1.191

Geometric mean variance (VG):

$$\mathrm{VG} = \exp\overline{((\ln X_0 - \ln X_\mathrm{p})^2)} \quad (16)$$

where X_0 is a CFD calculation quantity, X_p is the corresponding predicted quantity and the overbar indicates an average.

The elaboration of CFD calculation and predicted separation efficiency gave the statistical parameters values summarized in Table 4. Since the values of MG and VG are closed to 1, which is the perfect values of MG and VG, the predicted model could be considered consistent with the data from the CFD calculations.

3.2. Effect examinations of the operating parameters

The effect examinations of coded and uncoded factors are tabulated in Tables 5 and 6. A small probability value suggests that the influence of the factor is significant. When the probability value for a factor is greater than 0.05, it means that the influential degree of the factor is lower than the 95% confidence level. For some factors, the standard error is probably even bigger than the coefficient, resulting in a probability value approaching unity, which means the factor is very uninfluential. It shows that the probability values for those terms such as constant, five linear effects, one quadratic effect and two interaction effects are lower than 0.05. This suggests that these factors have significant influences on the objective function.

Table 5
Estimated regression coefficients for separation efficiency

Term	Coefficient	Standard error coefficient	*F*-Ratio	*P*-Value
Constant	0.7512	0.006301	119.222	0.000
α	−0.1275	0.002924	−43.601	0.000
H_1	0.0185	0.002924	6.314	0.000
H_2	0.0067	0.002924	2.276	0.033
D	−0.0443	0.002924	−15.158	0.000
v	0.0066	0.002924	2.248	0.035
$\alpha \times \alpha$	−0.036	0.01088	−3.311	0.003
$H_1 \times H_1$	0.0057	0.01088	0.522	0.607
$H_2 \times H_2$	0.008	0.01088	0.733	0.471
$D \times D$	0	0.01088	0.002	0.998
$v \times v$	−0.0103	0.01088	−0.949	0.353
$\alpha \times H_1$	−0.0009	0.003014	−0.299	0.768
$\alpha \times H_2$	0.0039	0.003014	1.294	0.209
$\alpha \times \mathrm{D}$	−0.0065	0.003014	−2.153	0.043
$\alpha \times v$	−0.014	0.003014	−4.647	0.000
$H_1 \times H_2$	0.0005	0.003014	0.164	0.871
$H_1 \times D$	0.0005	0.003014	0.16	0.875
$H_1 \times v$	−0.0053	0.003014	−1.767	0.091
$H_2 \times D$	0.0019	0.003014	0.628	0.536
$H_2 \times v$	−0.0015	0.003014	−0.506	0.618
$D \times v$	−0.0034	0.003014	−1.141	0.266

$R^2 = 98.9\%$, R^2 (adj) = 97.8%.

Table 6
Estimated regression coefficients for separation efficiency using data in uncoded units

Term	Coefficient	Term	Coefficient
Constant	1.95539	$\alpha \times H_1$	−0.000003
α	0.004491	$\alpha \times H_2$	0.000013
H_1	0.001046	$\alpha \times \mathrm{D}$	−0.000043
H_2	−0.02186	$\alpha \times v$	−0.00047
D	−0.0074	$H_1 \times H_2$	0.000005
v	0.182297	$H_1 \times D$	0.00001
$\alpha \times \alpha$	−0.00004	$H_1 \times v$	−0.00053
$H_1 \times H_1$	0.000057	$H_2 \times D$	0.000038
$H_2 \times H_2$	0.00008	$H_2 \times v$	−0.00015
$D \times D$	0.000001	$D \times v$	−0.00069
$v \times v$	−0.01033		

From the prediction model about the separation efficiency which was obtained based on response surface methodology, it can be seen that, this model not only takes the vane spacing and flue gas velocity into account, but also considers the vane height (including height of curve and upright region). The response surface for the separation efficiency can be visualized as a function of two different factors, which is presented in Fig. 4. The relationship between Y and D can be shown from Fig. 4a that with increasing the vane spacing, the separation efficiency decreases gradually. The reason is that increasing the vane spacing would extend the floating area of droplets. At the same time, the changing rate of the direction of flue gas becomes stable, which makes the follow property of droplets to flue gas better and easier for droplets to go through the vane. The relationship between Y and v can be shown from Fig. 4b. It is clear from the figure that, as the flue gas velocity is increased, the separation efficiency increases gradually. The reason is increasing the flue gas velocity would bring more inertial force, and droplets would change their moving direction rapidly and make them crash into the vane wall. Fig. 4 also shows the relationship between Y and α. The figure indicates that the separation efficiency decreases obviously when increasing the vane turning angle. This is because increasing the vane turning angle will decrease the centrifugal force of droplets.

3.3. Evolution of the response surface model

Because some terms in the model may turn out to be less significant, it would be adequate to dismiss those terms so that the model becomes more representative. Take Eq. (14) for instance, 9 out of the 15 model terms are regarded significant. Therefore,

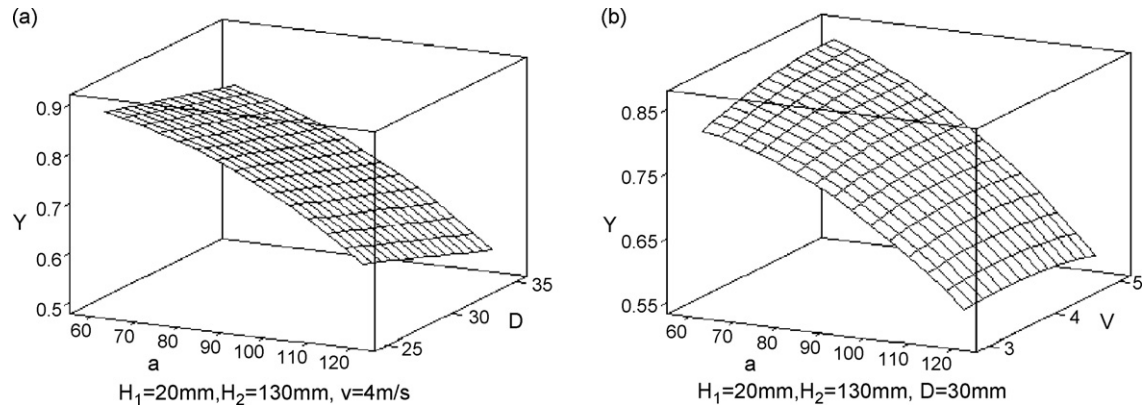

Fig. 4. (a and b) Response surfaces as a function of two different factors for separation efficiency.

Table 7
Corresponding analysis of variance of the evolutive quadratic model

Source	d.f.	Seq SS	Adj MS	*F*-Ratio	*P*-Value
Regression	8	0.648910	0.066742	185.25	0.000
Residual error	34	0.009451	0.000291		
Total	42	0.658361			

$R^2 = 96.9\%$, R^2 (adj) = 98.1%.

only these nine terms are kept to construct a new evolutive model as:

$$Y = 1.95847 + 0.004491X_1 + 0.001046X_2 - 0.02186X_3 - 0.0074X_4 + 0.182297X_5 - 0.00004X_1^2 - 0.000043X_1X_4 - 0.00047X_1X_5 \quad (17)$$

To evaluate the performance of the new model, original experimental data were regressed using Eq. (17) and proceeded with the analysis of variance. From Table 7, both the extremely small probability value and the high R^2 value suggest a good data fit. The fact that the R^2 value approaches the R^2 (adj) value is regarded as a result of dismissing insignificant factors in the model. Further more, as Eq. (17) could describe the effects of different geometries and operation conditions on the separation efficiency, the optimum design of the demister vane would be obtained according to the requirement of the separation efficiency.

4. Conclusions

A new prediction model of the separation efficiency was obtained based on response surface methodology by means of simulating gas flow fields of demister vane with different geometries and operating conditions. The results indicate that present prediction model is helpful in estimating the effects of different geometries and operation conditions on the demister's performance. According to different requirement of the separation efficiency, the optimum parameters of demisters can be advanced based on the present model.

Acknowledgements

Financial supports from the National Key Program of Basic Research in China (2005CB221202, 2006CB20030201 and 2006CB705806), the High-Tech Research and Development Program of China (2006AA05Z318, 2006AA020101) and the National Natural Science Foundation of China (50676021, 50606006) were sincerely acknowledged.

References

[1] G.A. Ekama, P. Marais, Assessing the applicability of the 1D flux theory to full-scale secondary settling tank design with a 2D hydrodynamic model, Water Res. 38 (3) (2004) 495–506.
[2] A. Prangnell, PET bottle flake filtration for fibers and spunbonds, Chem. Fibers Int. 52 (1) (2002) 40–42.
[3] M.R. Talaie, Mathematical modeling of wire-duct single-stage electrostatic precipitators, J. Hazard. Mater. B124 (2005) 44–52.
[4] J.K. Bradie, A.N. Dickson, Removal of entrained liquid droplets by wire-mesh demisters, Fluid mechanics and measurements in two-phase flow systems, Symp. by Thermodyn. and Fluid Mech. Group of Inst. Mech. Eng., and Yorkshire Br. of Inst. Chem. Eng., Inst. Mech. Eng. (Proc. 1969–1970, vol. 184, pt 3C), Univ. of Leeds, London, pp. 195–203.
[5] J. Claes, R. De Bruyne, Demisting with metal fibre webs and felts, Filtr. Sep. 13 (5) (1976) 494–501.
[6] K.S. Robinson, C. Hamblin, Investigating droplet collection in helices and a comparison with conventional demisters, Filtr. Sep. 24 (3) (1987), 166–167, 170–171.
[7] Y.N. Lebedev, V.G. Chekmenev, V.G. Vybornov, V. Sheinman, T.M. Zaitseva, High efficiency separators with string-type demisters, Chem. Technol. Fuels Oils 24 (1) (1988) 11–14.
[8] L.S. Sterman, V.A. Devyanin, Efficiency of droplet separation in louver-type demisters, Fluid Mech. Soviet Res. 17 (2) (1988) 41–45.
[9] F.N. Lang, J.Y. Chen, J.W. Wu, G.M. Zhao, Study on separation efficiency of a demister vane, Mach. Tool Hydraul. 5 (2003) 137–140.
[10] A.Y. Val'dberg, I.G. Kamenshchikov, A.V. Ogurtsov, Operation of fibrous demisters in galvanic industry, Khimicheskoe/Neftegazovoe Mashinostroenie 9 (2004) 44–45.
[11] S. Lim, Q.L. Zhou, T.M. Xu, S.E. Hui, A study of the type selection of mist eliminators with the help of $\Delta P - v - d_{cr}$ method, J. Eng. Thermal Energy Power 19 (2004) 575–578.
[12] L. Yang, S.H. Wang, X.M. Wang, Study on characteristics of a sulfur removal demister, Chin. J. Power Eng. 25 (2005) 289–292.
[13] H. Thomas, S. Hallvard, G.L. Henrik, Experimental characterisation of wire mesh demisters, in: AIChE Annual Meeting, Cincinnati, United States, 2005.

[14] Y. Wang, P.W. James, Calculation of wave-plate demister efficiencies using numerical simulation of the flow field and droplet motion, Chem. Eng. Res. Des. 76 (48) (1998) 980–985.
[15] Y. Wang, P.W. James, Assessment of an eddy-interaction model and its refinements using predictions of droplet deposition in a wave-plate demister, Chem. Eng. Res. Des. 77 (8) (1999) 692–698.
[16] A.V. Ogurtsov, A. Yu Val'dberg, S.N. Grishina, Calculation of efficiency of fibrous demisters in transient mode, Khimicheskoe/Neftegazovoe Mashinostroenie 4 (2003) 35–36.
[17] Y. Zhao, W. Hua, Y.J. Wang, S.C. Ma, J. Yan, Numerical simulation of separation efficiency of demisters with serrated baffles in wet flue gas desulfurization towers, Chin. J. Power Eng. 25 (2005) 293–297.
[18] S. Cooper, C.J. Coronellat, CFD simulations of particle mixing in a binary fluidized bed, Powder Technol. 151 (2005) 27–36.
[19] W.Q. Zhong, Y.Q. Xiong, Z.L. Yuan, M.Y. Zhang, DEM simulation of gas-solid flow in a spout-fluid bed, Chem. Eng. Sci. 61 (2006) 1571–1584.
[20] J.S. Ontko, Cyclones scaling revisited, Powder Technol. 87 (2) (1996) 93–104.
[21] Y.C. Lin, C.S. Chyang, Radial gas mixing in a fluidized bed using response surface methodology, Powder Technol. 131 (1) (2003) 48–55.
[22] D.M. Hasan, N.C. Melo, R.M. Fiho, Simulation and response surface analysis for the optimization of a three-phase catalytic slurry reactor, Chem. Eng. Process. 44 (3) (2005) 335–343.
[23] F.P. Qian, M.Y. Zhang, Study of the natural vortex length of a cyclone with response surface methodology, Comput. Chem. Eng. 29 (2005) 2155–2162.
[24] K. Hinkelmann, O. Kempthorne, Introduction to experimental design, in: Design and Analysis of Experiments, vol. 1, John Wiley and Sons, New York, 1994, pp. 87–94.
[25] G.E.P. Box, N.R. Draper, Empirical Model Building and Response Surfaces, John Wiley and Sons, New York, 1987, pp. 105–108.
[26] A.J. Hoesktra, Gas flow field and collection efficiency of cyclones, Ph. D. Thesis, Delft University of Technology, The Netherlands, 2000.
[27] W. Tao, Numerical Heat Transfer, Xi'an Jiaotong University Publications, Xi'an, 1988, pp. 207–211.
[28] C. Li, W. Ying, D. Peng, Newest development in numerical simulation theory for turbulent gas/solid two-phase flow, Power Syst. Eng. 18 (3) (2002) 19–20.
[29] H.P. Chen, Computational Fluid Dynamics, Water Conservancy and Hydroelectricity Publications, Beijing, 1995, pp. 97–103.
[30] M. Munoz, J. Arnaldos, J. Casal, E. Planas, Analysis of the geometric and radiative characteristics of hydrocarbon pool fires, Combust. Flame 139 (2004) 263–277.
[31] S. Sklavounos, F. Rigas, Simulation of coyote series trials—part: CFD simulation of non-isothermal LNG releases and comparison with box-model predictions, Chem. Eng. Sci. 61 (2006) 1434–1443.